Diffusion-Controlled Surfactant Adsorption Studied by Pendant Drop Digitization

Pendant drop tensiometry enhanced by video-image digitization is shown to be a useful tool for the experimental measurement of the relaxation in interfacial tension due to the adsorption of surfactant at a fluid interface. Using this method, profiles of the relaxation in surface tension of a diffusion-controlled, nonionic polyethoxy surfactant were measured. A diffusion coefficient was computed by comparing these profiles with numerical solutions of the bulk surfactant diffusion equation and a Frumkin equilibrium adsorption isotherm. This comparison was made for the entire relaxation period. This method establishes a more reproducible diffusion coefficient than current techniques that utilize only the short- or long-time parts of the relaxation spectrum. In addition, lower bounds on the kinetic constants for the sorption process are inferred for the polyethoxy surfactant used by comparing numerical solutions of mixed diffusion and surface kinetic transfer with the diffusion-limited result.

Shi-Yow Lin
Kevin McKeigue
Charles Maldarelli
Levich Institute for
Physicochemical Hydrodynamics
Department of Chemical Engineering
City College of New York
New York, NY 10031

Introduction

Pendant drop tensiometry, enhanced by video-image digitization, has emerged as a very accurate method for measuring the surface tension of fluid/fluid interfaces. In this method, video images of the silhouettes of pendant bubbles or drops are digitized to determine the interface loci. These loci are then compared with theoretical interfacial shapes generated by the solution of the Young-Laplace equation; the surface tension, which determines the theoretical constructs, is then varied until an optimum is achieved between the theoretical shape and the experimental loci (Rotenberg et al., 1983; Huh and Reed, 1983). Because this approach uses much more information about the drop shape, it is a much more accurate and reproducible method for measuring the surface tension than the classical selected plane technique of pendant drop tensiometry (Andreas et al., 1938) that uses only the diameters of a photographed drop at two locations.

The aim of this paper is to use pendant drop tensiometry enhanced by video-image digitization to examine the unsteady adsorption of surface-active molecules onto a fluid/fluid interface. When a fresh surface is created initially in a liquid medium containing surfactant molecules, surfactant in the sublayer adjacent to the surface kinetically adsorbs onto the interface. This depletes the concentration in the sublayer and gives rise in the liquid to a diffusive flux of surfactant toward the surface. The surface eventually becomes saturated with surfactant; as this driving force for kinetic adsorption becomes zero, the bulk phase returns to a uniform concentration of surfactant. The adsorption of surfactant onto the interface lowers the interfacial tension, and therefore the coupled sorptive and diffusive process can be studied experimentally by measuring the interfacial tension relaxation.

The experimental measurement of surface tension relaxation due to surfactant adsorption and the calculation of diffusion coefficients or sorptive kinetic constants from these measurements have been undertaken using many techniques. These are of three types:

1. Methods involving hydrodynamic flow
2. Static techniques involving no fluid convection
3. Surface oscillation techniques.

Methods involving flow are useful for studying adsorption processes that occur on time scales of the order of milliseconds to seconds, while static methods are most accurate on scales of the order of seconds to hours. Oscillation techniques can resolve time scales of the order of milliseconds to several minutes.

Some of the methods involving convection are:

- Oscillating jet technique (Defay and Hommelen, 1958; Hansen et al., 1958; Thomas and Potter, 1975)

Correspondence concerning this paper should be addressed to C. Maldarelli.

• Maximum bubble pressure method (Bendure, 1971; Kloubek, 1972; Fainerman and Lylyk, 1982; Hua and Rosen, 1988)

• Free falling film (Balbaert et al. 1987) or inclined plate technique (Van den Bogaert and Joos, 1979)

• Drop volume or weight method (Pierson and Whitaker, 1976; Van hunsel et al., 1986)

• Funnel (reversed) method (Van hunsel and Joos, 1989).

The convection differs in each of these techniques. For the oscillating jet, the fluid issues through an orifice, for the inclined plane method liquid flows with a free surface down a plane, and for the maximum bubble pressure and drop volume methods the surfactant solution expands radially in the vicinity of the interface. In these methods, diffusion coefficients or kinetic constants are generally obtained by: (i) identifying an exposure time t, for which the surface has been in contact with the surfactant solution; (ii) measuring the surface tension for that time; and (iii) computing the adsorption theoretically by solving the surfactant mass transfer to the interface. In most cases, convection is ignored altogether, and theoretical solutions used to compare with the data are the planar diffusion-controlled result of Ward and Tordai (1946) (and only for short and long contact times). For the maximum bubble pressure and drop weight methods, however, theoretical equations have been constructed to account for the radial convection induced by the drop growth (Pierson and Whitaker, 1976; Fainerman, 1980; Joos and Rillaerts, 1981). Theoretical solutions of these convection equations have been compared with short-time experimental data to obtain diffusion coefficients (Joos and Rillaerts, 1981).

The static methods used for the measurement of the surface tension relaxation are the Whilhelmy plate and Du Nouy ring method (Lunkenheimer and Wantke, 1981), the static drop volume method (Van hunsel and Joos, 1987), and the pendant drop technique (Girault et al., 1982, 1984). These have the advantage that surfactant transfer in the bulk can be described accurately by diffusion alone. Relaxation data from the plate and ring methods (Miller and Lunkenheimer, 1986) and the static drop volume technique (Miller and Schano, 1986) have been compared with the short-time solution of Ward and Tordai to determine diffusion coefficients. Intermediate times were compared (Miller and Lunkenheimer, 1986) approximately by regarding the intermediate-time solution for the surface concentration as linear in log t and deducing the diffusion coefficient from the shift of the experimental data for the adsorption (plotted as log t and regarded as linear) from the theoretical curve.

Primary surface oscillation techniques are the longitudinal wave method of Lucassen (Lucassen and van den Tempel, 1972; van den Tempel and Lucassen-Reynders, 1983; Noskov and Vasil'ev, 1988) and the oscillating bubble technique (Lunkenheimer et al., 1984, 1990). The longitudinal wave method, when undertaken using small lateral oscillations of the interface creating small deviations from equilibrium, has the advantage that a perturbative analytical solution can be developed for the oscillation of the surface tension as a function of the surfactant mass transfer and hydrodynamic motion. Using this method, diffusion-controlled adsorption was demonstrated for decanoic acid and several surfactants of the ethylene oxide adduct type for a range of frequencies of 10^{-2} and $10^{-1}s^{-1}$ (Lucassen and van den Tempel, 1972; van den Tempel and Lucassen-Reynders, 1983).

Before the advent of video digitization, classical pendant drop tensiometry was not used to obtain surface tension relaxation profiles because sequential photography is cumbersome. With video digitization, however, sequential profiles in time can readily be obtained and stored. The goals of this paper are twofold. The first is to demonstrate that by sequential digitization, video-enhanced pendant drop tensiometry can be used to accurately determine surface tension relaxation profiles. The second is to employ a diffusion-controlled test surfactant system (Triton X-100 in water) and to show how relaxation profiles determined by this method can be used to evaluate the diffusion coefficient and to set lower bounds on the kinetic constants. In this regard, the coupled sorption and diffusion equations are solved numerically and compared with the experimental profiles for the entire length of the relaxation time. As will be shown, this allows for a more reliable and reproducible measure of the diffusion coefficient.

This paper first details the experimental apparatus used for the video-enhanced pendant drop tensiometry measurements and the algorithm from which the surface tension is computed. Next, the theoretical framework for the surfactant mass transfer process and the numerical solution procedure are discussed. Subsequently, the experimental relaxation profiles are compared with the diffusion-limiting mass transfer solutions, which leads to the computation of the diffusion coefficient. Finally, the reasons for the discrepancy between the experimental and theoretical relaxation profiles are explained.

Experimental Measurement Technique

Apparatus

The equipment shown in Figure 1 is used to create a silhouette of a pendant drop, to video-image the silhouette, and to digitize

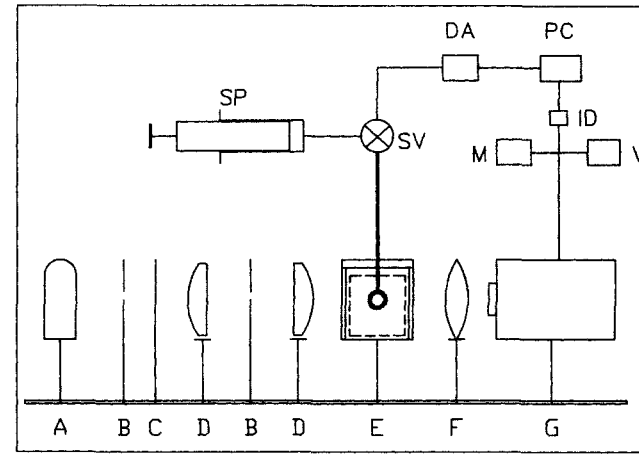

Figure 1. Pendant drop tensiometry apparatus and video-image digitization equipment.

A = light source
B = pin hole
C = filter
D = planoconvex lens
DA = D/A data translation card
E = thermostatic chamber, quartz cell and suspending needle
F = objective lens
G = video camera
ID = image digitizer
M = monitor
PC = IBM-PC AT
SP = syringe and syringe pump
SV = solenoid valve
V = video recorder

the image. The equipment consists of an image forming and recording system, a drop-forming system, and a video-image profile digitizer.

The image forming and recording system consists of a light source (a halogen lamp with constant light intensity), a plano-convex lens system for producing a collimated beam, a quartz cell enclosed in a thermostatically controlled chamber, an objective lens (effective focal length 60 mm, f/# 7.1), and a solid-state video camera (CCD-71 series, Dage-MIT Inc.). The drop onto the active area of the camera is magnified approximately $\times 1.5$. The drop-forming system consists of a stainless-steel inverted needle (ID = 0.41 mm), which is connected to the normally closed port of a three-way miniature solenoid valve (Lee Co.) via 1/16 in. (1.6 mm) ID teflon tubing. The common port of the valve is connected by the same teflon tubing to an gas-tight Hamilton syringe placed in a syringe pump (Sage Instruments). The valve is controlled by the output signal of a D/A Data Translation card (DT2801) installed on an IBM-PC AT. The video-image digitizer (DT 2861 Arithmetic Frame Grabber, Data Translation), also installed on the backplane of the AT, digitizes the picture into 480 lines $\times$ 512 pixels and assigns to each one a level of grey with an eight-bit resolution. Note that the maximum rate, with which an image can be digitized, is 1/30 of a second.

An edge detection routine was devised in the following way. An example of an original digitized image is shown in Figure 2. Figure 2 shows a change in the grey level from the black inside (0 level) to the bright outside (255 level) in a few pixels. This change is not a step increase from 0 to 255, but is continuous. The fact that it is not a step increase can in principle be attributed to the fact that the light is not exactly parallel and the refraction of light around the bubble. However, the calibration images of the stainless steel-ball (see below) also exhibited a similar grey level variation. Since refraction in this case is minimal, the grey level change in both the bubble and sphere cases may be attributed principally to the imperfection in the light source. It is probable that nonparallel rays are randomly distributed; such a distribution will create, around the true edge

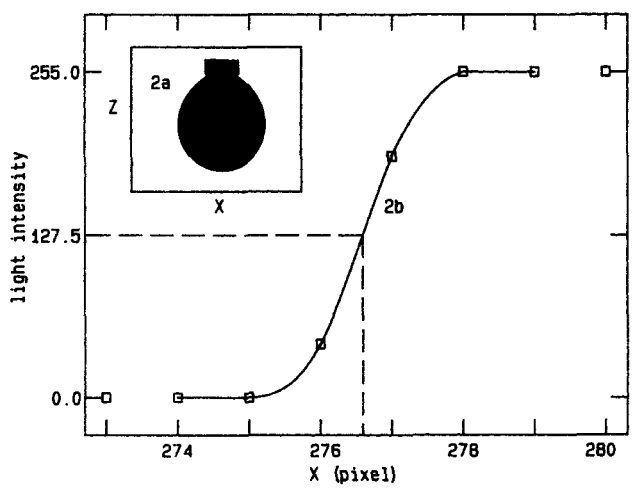

Figure 2. a. Sample digitized image of air/water interface: R_o = 0.944 mm. b. Edge location determination from digitized image profile.

of the drop, a symmetric distribution in the grey level. A close inspection of Figure 2 indicates that the variation is symmetric around 127.5, and therefore the true edge should be located by identifying the symmetry point. It also indicates that in the immediate vicinity of 127.5, the change is almost linear. Therefore, the drop edge is obtained by first interpolating a straight line between the two points that bound the grey level 127.5. The edge is defined as the x or z position which, for the interpolated line, corresponds to an intensity of 127.5. Note that the location procedure is performed in the coordinate direction, in which the normal to the surface has the larger component. Thus, near the apex the edge location is done along the z direction, while near the sides of the drop it is done along the x direction.

The image forming system was calibrated by digitizing a stainless-steel sphere with a known diameter of 1.581 mm $\pm$ 1 μm. The coordinates of the digitized sphere were processed to calculate the average length between pixels along a row and along a column. The calibration procedure yielded values of 0.10096 pixel/μm horizontally and 0.12817 pixel/μm vertically. The origin of this asymmetry is in the positioning of the active picture elements on the pickup area of the CCD camera. The camera used (CCD-71 from Dage Instruments, Inc.) has a pickup area, 8.8 mm (horizontal) and 6.6 mm (vertical), and 510 picture elements arranged horizontally and 492 vertically. Thus, the number of pixels per unit length is smaller in the horizontal direction.

Materials and methods

The surfactant that was dissolved in the aqueous phase was Triton X-100, $CH_3C(CH_3)_2CH_2C(CH_3)_2C_6H_4(OCH_2CH_2)_nOH$ ($n = 9 - 10$), obtained from Aldrich Chemical Co. and used without modification. The water, with which the aqueous solutions were made, was purified via a Millipore water purification system, with the output water having a specific conductance of 0.056 micromho/cm (0.056 μS/cm). The pendant drop phase is either air or fluorocarbon oil (FC-43, Sigma Co.). Acetone (HPLC grade) used to verify the measurement was obtained from Fisher Scientific Co.

The experimental protocol was as follows. The quartz cell was initially filled with the aqueous solution, and the drop forming needle was positioned in the cell in the path of the collimated light beam. At this point, the solenoid valve was not energized. The syringe pump was turned on, and the fluid in the syringe (either air or fluorocarbon oil) was allowed to pass through the normally open port of the valve. Via input from the keyboard, the D/A card energized the valve and allowed the fluid to pass through the needle, thereby forming a bubble of air or a drop of oil. The valve was then closed (also by input from the keyboard) when the drop achieved a diameter of approximately 2 mm. The drop so created is one of constant mass, and the change in volume, as the surface tension relaxes, is only a few percent over a time period of 2–3 h. The time required to create an air bubble of this size is $\approx$ 2 s and for the oil drop $\approx$ 4 s. Sequential digital images were then taken of the drop, first at intervals of approximately 1 s and then later in intervals of the order of tens of seconds. All experiments were undertaken at 22.0 $\pm$ 0.5°C. After the surface tension relaxation was complete, the images were processed to determine the drop edge coordinates.

Surface tension calculated from the drop profile

The classical Laplace equation relates the pressure drop across a curved interface

$$\gamma\left(\frac{1}{R_1}+\frac{1}{R_2}\right)=\Delta P \tag{1}$$

where γ is the boundary tension, R_1 and R_2 are the two principal radii of curvature of the surface, and ΔP is the pressure difference across the interface. For the pendant drop geometry, Eq. 1 can be recast as a set of three first-order differential equations for the spatial positions x and z and turning angle ϕ of the interface as a function of the arc length s. Nondimensionalizing by the radius of curvature at the apex ($x' = x/R_o$, $z' = z/R_o$, and $s' = s/R_o$), the first-order equations have the following form (Rotenberg et al., 1983):

$$\frac{d\phi}{ds'}=2+Bz'-\frac{\sin\phi}{x'}$$

$$\frac{dx'}{ds'}=\cos\phi$$

$$\frac{dz'}{ds'}=\sin\phi \tag{2}$$

where B defines the Bond number or capillary constant and is given by $(\Delta\rho g R_o^2)/\gamma$, and $\Delta\rho$ is the density difference between the fluids and g is the gravitational acceleration constant. The equations are subject to the boundary conditions $x'(0) = z'(0) = \phi(0) = 0$. Equation 2 is integrated by using a fourth-order Runge-Kutta scheme initialized with the approximate solution $z' = [2/(-B)^{1/2}][1 - J_o(x)]$, which is valid near the apex where $\phi \ll 1$ (Huh and Reed, 1983). (Here $J_o(x)$ is the Bessel function of the first kind.)

The surface tension is computed from the data and the theoretical curve in the following way. An objective function E is defined as the sum of squares of the normal distance d_n between the measured points u_n and the calculated curve v obtained from the integration of Eq. 2 (i.e., $E = \sum_{n=1}^{N}[d_n(u_n, v)]^2$; N is the total number of experimental points). The objective function depends on four unknown variables, X_o and Z_o, the actual location of the apex, R_o and B. To obtain the optimum congruence between the theoretical curve and the data points, the objective function is minimized with respect to the four parameters ($\partial E/\partial q_i = 0$, $i = 1, 2, 3, 4$). Minimization equations are solved by applying directly the Newton-Raphson method, and from the optimum values of R_o and B the tension γ can be computed.

From the data sets, there are approximately 600 measured coordinates of the drop edge for each image, with $R_o \approx 1$ mm. To obtain d_n for each point, first a theoretical curve consisting of 6,000 points is generated, and then d_n is computed as the distance from the experimental point to the closest of the discrete theoretical points. The Newton-Raphson procedure is arrived at in the following way. X_o is initially guessed as the centroid of the 600 x location data points, and Z_o as the average of the three lowest z coordinates. Initial guesses for R_o and B are obtained by using the selected plane method for pendant drops (Andreas et al., 1938; Ambwani and Fort, 1979). The equatorial diameter (d_e) and the diameter (d_s) in a selected plane at a distance d_e from the apex to the drop are obtained from the raw data. By integrating Eq. 2 for different values of B, graphs can be constructed of B, d_e/R_o, and $B(d_e/R_o)^2$ $(=-H)$ as a function of d_s/d_e $(=S)$. The Misak correlation (Misak, 1968) correlates $1/H$ as a function of S. As S is known from the raw data, H and therefore γ can be obtained. A separate correlation is constructed of B as a function of S; with the knowledge of γ, an initial guess for R_o can be obtained. Two to five iterations are necessary for the program to converge, and the standard deviation of the distance between a measured point and the calculated curve is about 0.1 pixel (≈ 1 μm). Error analysis and curve fitting of a typical run are shown in Figures 3a and 3b.

An estimate for the error involved in the measurement of the surface tension may be constructed as follows. The error in the location of the edge at each edge coordinate may be estimated to be 0.1 pixel, since it is the standard deviation of the exact theory (Eq. 2) from the experimental data. A random number generator is used to create a set of random numbers with an average value of zero and a standard deviation of 0.1 pixel. The program that computes the surface tension as a function of the edge coordinates is run with a set of data, in which each edge coordinate of a sample run is perturbed by an element of the random number set. The assignment of the perturbation was done such that in the region surrounding the apex of the drop the z location is perturbed, while the x coordinate is perturbed for the remaining data points. The results for several random number sets indicate a deviation from the computed value of γ for the unperturbed data set of less than $\pm$ 0.1 mN/m.

This measurement technique was verified by measuring the surface tension of air/water and air/acetone. The values of the surface tension obtained from this work as compared with that reported in the literature (Weast, 1973) are shown in Table 1. A conservative estimate for the reproducibility of these measurements is $\pm$ 0.1 mN/m; as this is in agreement with the error estimate, a value of 0.1 mN/m may be assigned to the accuracy

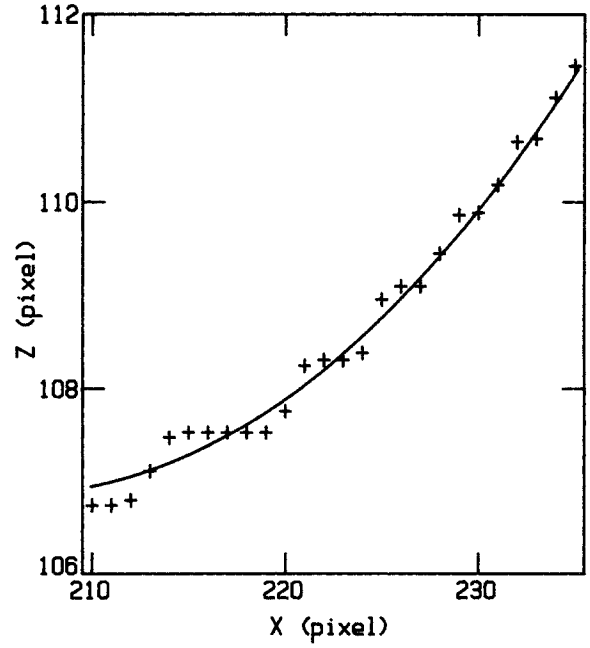

Figure 3a. Young-Laplace fitting of the region near apex for the sample digitized image of Figure 2a.

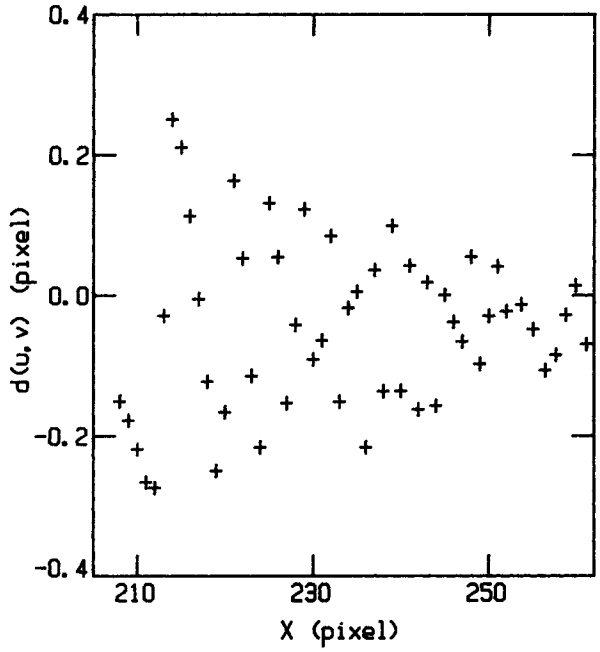

Figure 3b. Error analysis of sample image: maximum error = 0.28% (of R_o); standard error = 0.13% (of R_o).

of the measurements reported here. With this bound, the values of γ measured for air/water and air/acetone agree with the literature values.

In unsteady experiments, the relaxation in the surface tension causes the bubble shape to elongate. This elongation is considerable: As an example consider a relaxation in surface tension from 70 to 49 mN/m; the edge data for such a relaxation shows that the location of the apex moves 21 pixels in the z direction. Note that this change is much larger than the 0.1 pixel standard deviation distance between the experimental points and the fitting curve.

Theoretical framework

Discussed in this section are the theoretical framework describing the unsteady adsorption of surfactant onto a pendant drop interface and its effect on the interfacial tension. The pendant drop is treated as a spherical drop surrounded by an infinite medium containing a surfactant (Mysels, 1982; Adamczyk and Petlicki, 1987). The surfactant is assumed not to dissolve into the drop phase. Mass transfer to an initially clean drop surface is described by Fick's law,

$$D\frac{1}{r^2}\frac{\partial}{\partial r}\left(r^2\frac{\partial C}{\partial r}\right)=\frac{\partial C}{\partial t} \qquad (r>b,\ t>0) \tag{4}$$

Table 1. Verification of Measurement

	γ (mN/m)	
	This Study	Literature
Air/Water	72.5 ± 0.1	72.44
Air/Acetone	23.6 ± 0.1	23.45

(in which the diffusion is assumed to be spherically symmetric and convection effects are neglected) with boundary and initial conditions

$$C(r,t)=C_o \qquad (r>b,\ t=0)$$
$$C(r,t)=C_o \qquad (r\to\infty,\ t>0)$$
$$\frac{d\Gamma(t)}{dt}=D\left(\frac{\partial C}{\partial r}\right) \qquad (r=b,\ t>0)$$
$$\Gamma(t)=0 \qquad (t=0)$$

where r and t are the spherical radial coordinate and time, D denotes the diffusion coefficient, $C(r, t)$ the bulk concentration, $\Gamma(t)$ the surface concentration, b the drop radius, C_o the concentration far from the drop. By the Laplace transform, the solution to the above set of equations can easily be formulated in terms of the unknown subsurface concentration $C_s(t) = C(r = b, t)$:

$$\Gamma(t)=\frac{D}{b}\left[C_o t-\int_0^t C_s(\tau)d\tau\right]+2\left(\frac{D}{\pi}\right)^{1/2}\left[C_o\sqrt{t}-\int_0^{\sqrt{t}}C_s(t-\tau)\,d\sqrt{\tau}\right] \tag{5}$$

or in nondimensional form:

$$\Gamma'(t')=\frac{h}{b}\left[t'-\int_0^{t'}C_s'(\tau)d\tau\right]+\left(\frac{2}{\sqrt{\pi}}\right)\left[\sqrt{t'}-\int_0^{\sqrt{t'}}C_s'(t'-\tau)\,d\sqrt{\tau}\right]$$

where $\Gamma' = \Gamma/\Gamma_o$ (Γ_o is the equilibrium surface concentration at the bulk concentration C_o), $C_s' = C_s/C_o$, $t' = t/(h^2/D)$ and $h = \Gamma_o/C_o$ is the adsorption depth. Note that this result differs from the classical solution of Ward and Tordai (1946) for the unsteady diffusion toward an initially clean planar surface by the extra term $(h/b)\ [t' - \int_0^{t'} C_s'(\tau)d\,\tau]$, which accounts for the interface curvature. It will be shown later that this term plays an important role for long times.

To complete the solution for the surface concentration, the sorption kinetics must be specified. The model used here utilizes the Langmuir formalism, in which on a liquid surface there is a finite number of adsorption sites, as for a solid surface. The adsorption rate is proportional to the concentration of surfactant C_s just below the surface and the fraction of surface area unoccupied, while the desorption rate is proportional to the fraction of the area covered by adsorbed surfactants. Thus,

$$\frac{d\Gamma}{dt}=\beta\exp\left(-E_a/RT\right)C_s(\Gamma_\infty-\Gamma)-\alpha\exp\left(-E_d/RT\right)\Gamma \tag{6a}$$

where β, α, E_a, E_d are the preexponential factors and the energies of activation for adsorption and desorption, respectively, Γ_∞ is the saturated surface concentration, T is the temperature, and R the gas constant.

The activation energies for adsorption and desorption are assumed to depend on the surface coverage, and here a linear

dependence is used (Guzman et al., 1986). Thus,

$$E_a = E_a^0 + \nu_a \Gamma$$
$$E_d^0 = E_d^0 + \nu_d \Gamma \tag{6b}$$

where E_a^0, E_d^0, ν_a, and ν_d are constants. At equilibrium, the time rate of change of Γ vanishes and gives

$$\Gamma = \frac{\Gamma_\infty C_s}{a \exp(k\Gamma/\Gamma_\infty) + C_s} \tag{7}$$

where

$$a = \frac{\alpha \exp(-E_d^0/RT)}{\beta \exp(-E_a^0/RT)} = \bar{\alpha}/\bar{\beta}$$

and

$$k = (\nu_a - \nu_d)\Gamma_\infty/RT$$

Equation 7 is the Frumkin adsorption isotherm (Borwankar and Wasan, 1983), which relates the subsurface and surface concentrations. Equation 7 becomes the Langmuir adsorption isotherm when $\nu_a = \nu_d = k = 0$.

When the surfactant solution can be considered ideal, the Gibbs adsorption equation $d\gamma = -\Gamma RT\, d \ln C$ and the equilibrium isotherm allow for the calculation of the surface tension explicitly in terms of Γ:

$$\gamma_o - \gamma = -\Gamma_\infty RT [\ln(1-y) - \tfrac{1}{2} k y^2]$$
$$= \Gamma_\infty RT [y + \tfrac{1}{2}(1+k)y^2 + \tfrac{1}{3} y^3 + \tfrac{1}{4} y^4 + \ldots] \tag{8}$$

where $y = \Gamma/\Gamma_\infty$, and γ_o is the clean surface tension. Equation 8 is the Frumkin equation (Lucassen-Reynders and van den Tempel, 1964), with an extra $ky^2/2$ term on the righthand side representing the linear dependence of activation energies for adsorption and desorption on the surface converge. Equation 8, of course, is strictly true only at equilibrium. By fitting equilibrium data of the surface tension as a function of the bulk concentration using Eqs. 7 and 8, the equilibrium constants k and a, and the maximum coverage Γ_∞ can be obtained. It is also assumed here for the nonequilibrium relaxation process that Eq. 8 gives the unsteady surface tension $\gamma(t)$ as a function of the unsteady coverage $\Gamma(t)$ obtained from the solution of the transport equations (Eqs. 5 and 6).

Equations 5 and 6 must be solved numerically. The technique used is similar to that used by Miller and Kretzschmar (1980) and is described as follows. First, the convolution integral of C_s in Eq. 5 is integrated by first partitioning the interval $(0, t)$ into intervals of size δ in time and integrating separately each interval by assuming a linear relation in time for C_s.

$$\int_0^t C_s(t-\tau)/\sqrt{\tau}\, d\tau = \sum_{i=0}^{n-1} \int_{i\delta}^{(i+1)\delta}$$
$$\cdot \{[C((n-i-1)\delta) - C((n-i)\delta)]\tau/\delta$$
$$+ [(i+1)C((n-i)\delta) - iC((n-i-1)\delta)]\}/\sqrt{\tau}\, d\tau$$
$$= \left[\frac{4}{3} C(n\delta) + \frac{2}{3} C((n-1)\delta)\right]\sqrt{\delta}$$
$$- \sum_{i=1}^{n-1} \frac{2}{3} [C((n-i)\delta) - C((n-i-1)\delta)]$$
$$\cdot [(i+1)^{3/2} - i^{3/2}]1\delta^{1/2}$$
$$+ \sum_{i=1}^{n-1} 2[(i+1)C((n-i)\delta)$$
$$- iC((n-i-1)\delta)][(i+1)^{1/2} - i^{1/2}]\sqrt{\delta} \tag{9}$$

After integration, Eq. 5 is of the form

$$C_s(t_n) = b_1 \Gamma(t_n) + b_2 \tag{10}$$

where $t_n = n\delta$ and the subscript on C is dropped in Eq. 9.

The next step in the numerical procedure depends on whether the sorption kinetics is finite or not. If the kinetics were infinite and the mass transfer were only diffusion-controlled, then $\Gamma(t)$ is calculated by substituting C_s in Eq. 10 into Eq. 7. After that, the dynamic surface tensions are obtained from Eq. 8. If, however, sorption kinetics were finite, then the equation $C_s(t_n) = b_1\Gamma(t_n) + b_2$ must be solved simultaneously with Eq. 6 to obtain $\Gamma(t_n)$, and finally $\gamma(t_n)$ from Eq. 8. Equation 6 is solved by assuming that $C_s(t)$ is constant in each time interval, and then, for that interval, integrating Eq. 6 numerically.

Results

Relaxations in the surface tension due to Triton X-100 adsorption were measured at the air/water interface. The data were recorded from one second up to a few hours. Figure 4 shows representative dynamic surface tension profiles (against air) of Triton X-100 aqueous solutions at six different bulk concentrations. The reproducibility of these profiles is shown in Figure 5, together with the results of several pendant bubbles at three fixed concentrations. To demonstrate the applicability of the

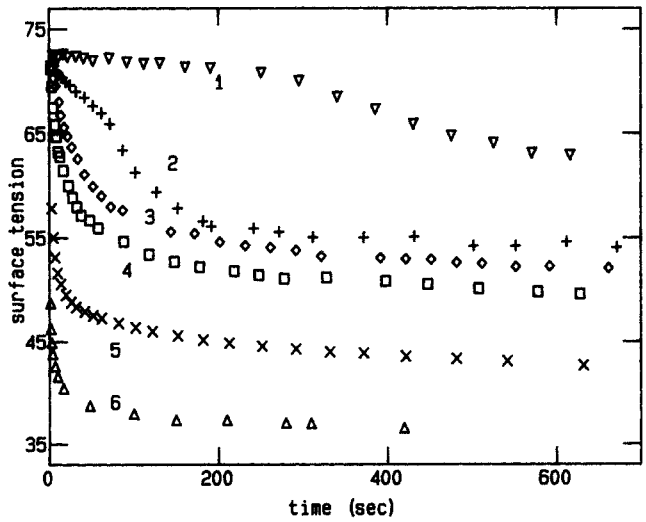

Figure 4. Representative dynamic surface tensions of Triton X-100 solutions.

C_o = (1) 1.55×10^{-9}, (2) 9.89×10^{-9}, (3) 1.55×10^{-8}, (4) 2.32×10^{-8}, (5) 4.64×10^{-8} and (6) 1.24×10^{-7} mol/cm^3 (γ = mN/m)

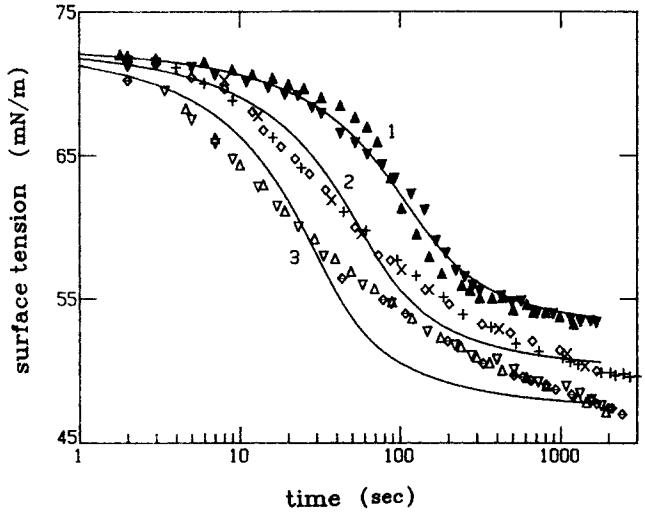

Figure 5. Dynamic surface tensions of Triton X-100 solutions and theoretical profiles.

C_o = (1) 9.89×10^{-9}, (2) 1.55×10^{-8}, and (3) 2.32×10^{-8} mol/cm^3; $D = 2.6 \times 10^{-6}$ cm^2/s. Each symbol represents a separate bubble (γ = mN/m)

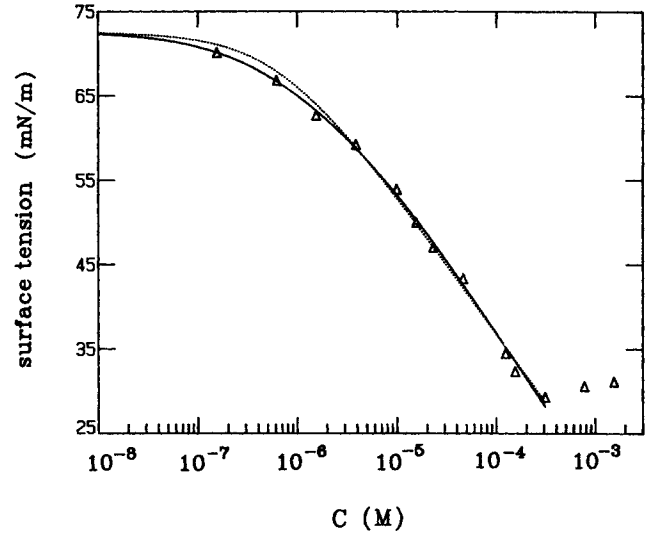

Figure 7. Equilibrium surface tension for air/Triton X-100 aqueous solution.

Theoretical fitting by Eqs. 7 and 8: Frumkin isotherm (———) and Langmuir isotherm (·····) (γ = mN/m)

method to liquid/liquid interfaces, relaxation profiles at the fluorocarbon oil/water interface were obtained at two different concentrations of Triton X-100 solutions, Figure 6.

The equilibrium surface tensions for aqueous Triton X-100 solutions at the aqueous/air interface are extracted from the long-time asymptotes in Figure 4, and are plotted as the symbols in Figure 7. The isotherm described by Eqs. 7 and 8 can be fitted to the data by varying the values of Γ_∞, a and k. The results are given as the solid line in Figure 7; the constants are $\Gamma_\infty = 3.20 \times 10^{-10}$ mol/cm^2, $a = 3.11 \times 10^{-10}$ mol/cm^3, and $k = 2.52$. From the figure, the CMC for Triton X-100 at the aqueous–air interface can be inferred to be approximately 2.3×10^{-7} mol/cm^3.

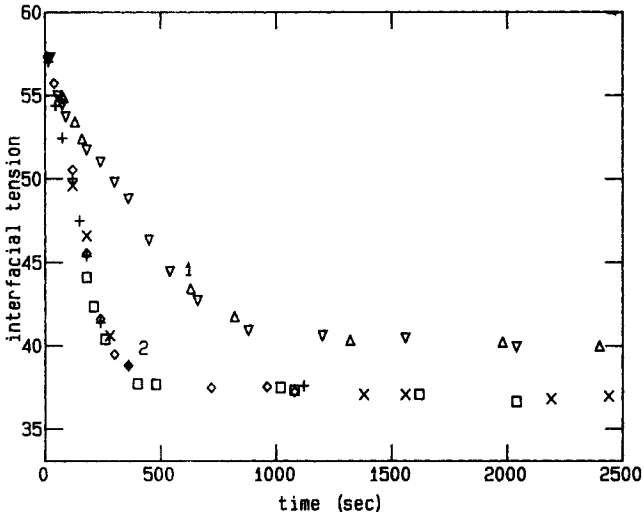

Figure 6. Dynamic interfacial tensions of Triton X-100 aqueous solution against fluorocarbon oil.

C_o = (1) 6.18×10^{-10}, (2) 1.55×10^{-9} mol/cm^3 (γ = mN/m)

It should be noted that by taking into account the fact the energies for adsorption and desorption depend on the surface coverage (Eq. 6b), a much better fit of the equilibrium data is achieved at the low concentrations than the $k = 0$ von Szyszkowski's equation [$\gamma = \gamma_o - RT\Gamma_\infty \ln(1 + C/a)$]. The von Szyszkowski's fit is given as the dotted line in Figure 7 with constants $\Gamma_\infty = 2.91 \times 10^{-10}$ mol/cm^2 and $a = 6.62 \times 10^{-10}$ mol/cm^3. From the definition of k, a positive value may be interpreted in the following way: at increasing surface coverage, work is required to insert additional surfactant molecules onto the surface, and therefore the desorption rate increases relative to that of adsorption.

If the relaxation of Triton X-100 were assumed to be diffusion-controlled, Figures 4 and 5 may be used to determine a diffusion coefficient for the surfactant molecule in the aqueous phase. A candidate profile for this determination must have certain characteristics. The first is that the relaxation should not be too fast. Since the time scale for the diffusional relaxation process is of the order h^2/D, higher concentrations yield faster relaxations. From Figure 4 it is clear that the profiles of the two highest concentrations (i.e., 4.64×10^{-8} and 1.24×10^{-7} mol/cm^3) fall off too rapidly for any accurate analysis. Second, the asymptote of the relaxation should differ substantially from the clean surface tension, so that errors in the measurements at particular times remain small in comparison to the overall change in the surface tension. Since this requires the bulk concentration not to be too small, the three middle bulk concentrations are used to determine the diffusion coefficient.

Theoretical diffusional relaxations, described previously, are given in Figure 5 for the three middle concentrations of Figure 4. To obtain these curves, the radius of the drop (b) was set equal to the curvature R_o at the apex. In addition, these curves were obtained using a value of 2.6×10^{-6} cm^2/s for the diffusion coefficient, a value which minimizes, for all these concentrations, the difference between the theoretical and the experimental profiles. To examine the sensitivity of this determination of D, Figure 8 graphs the standard deviation as a function of the

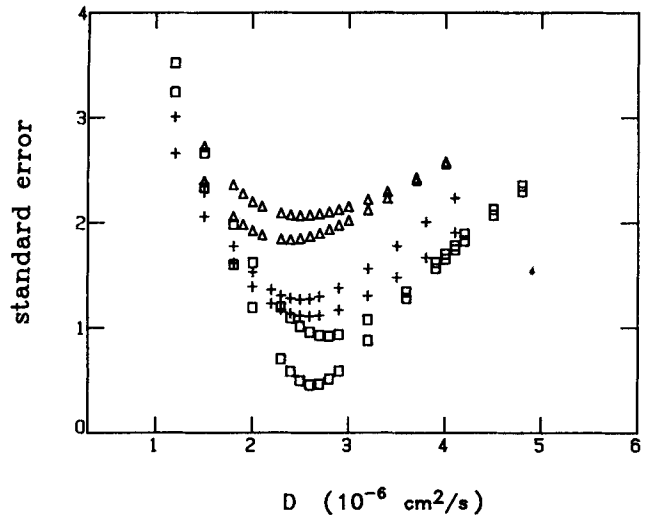

Figure 8. Sensitivity of the standard error of theoretical solution and experimental data to the value of diffusion coefficient.

(□) 9.89×10^{-9}, (+) 1.55×10^{-8}, (△) 2.32×10^{-8} mol/cm³

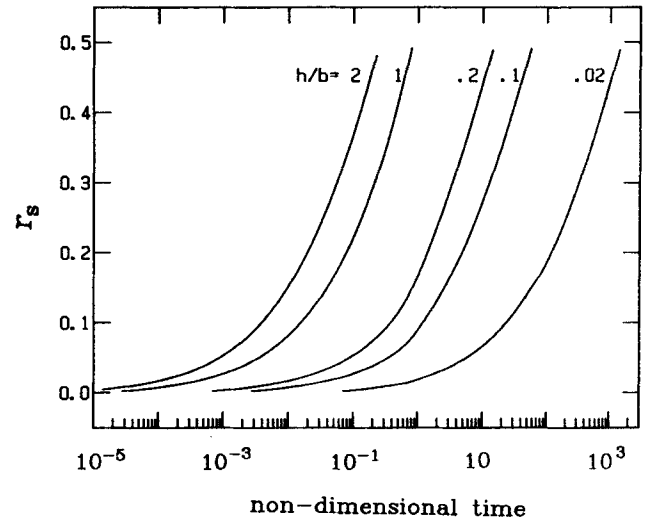

Figure 9. Effect of the spherical term of Eq. 5 in diffusion-controlled adsorption process.

h/b = (a) 2, (b) 1, (c) 0.2, (d) 0.1, and (e) 0.02 with b = 1 mm, $\Gamma_\infty = 2.91 \times 10^{-10}$ mol/cm² and $a = 6.62 \times 10^{-10}$ mol/cm³

diffusion coefficient for two pendant bubbles at each of the three bulk concentrations. From this study, the average value of D is 2.6×10^{-6} cm²/s, and the standard deviation is 0.14×10^{-6} cm²/s. A value of D of $2.6 \pm 0.3 \times 10^{-6}$ cm²/s (the accuracy being estimated by twice the standard deviation) compares favorably with the range of 1.9–2.3 $\times 10^{-6}$ cm²/s obtained for a similar concentration range by Van hunsel et al. (1986) using the drop volume method.

Two important characteristics of these theoretical profiles and their relationships with the experimental data should be noted.

First, for the spherical model it could be argued that since the ratio of the adsorption depth to the drop radius is small for the three concentrations used for theoretical matching ($h/b = 0.36$, 0.24, and 0.16 for $C_o = 9.89 \times 10^{-9}$, 1.55×10^{-8}, and 2.32×10^{-8} mol/cm³, respectively), only the planar Ward and Tordai expression is necessary. Figure 9 shows the ratio (r_s) of the spherical term $\{(h/b)\,[t' - \int_0^{t'} C'_s(\tau)d\tau]\}$ to that of the entire expression for $\Gamma'(t)$ for diffusion-controlled adsorption using a Langmuir isotherm. In the nondimensional formulation, two dimensionless parameters appear, $h/b = (\Gamma_\infty/C_o)/b$ and C_o/a; in the curves of Figure 9, a, b, and Γ_∞ are held constant, and C_o is varied generating different values for h/b (and C_o/a). The curves indicate that for times much less than h^2/D ($t' \ll 1$), the planar result is sufficient even for a relatively large h/b. More importantly, however, they indicate that no matter how small the value of h/b, there are long nondimensional times for which the spherical term becomes important. This reflects the physical fact that for long enough time, the diffusional flux to the interface lowers the bulk concentration far outside the adsorption depth, and the process is thereby affected by the bulk geometry. In the experimental relaxations which are fitted, h/b is of the order of 10^{-1}, and therefore the spherical term becomes important ($r_s > 0.1$) after one nondimensional unit or 10^2 s (since h^2/D is of the order of 10^2 s). Figure 5 shows that there are many data points after 10^2 s, and therefore the use of the planar result to fit these points would yield values of the diffusion coefficient which would be too large, because the spherical term is positive. For example, using the planar result, the analogue of Figure 8 yields a value of $3.4 \pm 0.5 \times 10^{-6}$ cm²/s for the diffusion coefficient of the Triton X-100 molecule.

Second, the diffusion fits of Figure 5 concerns the possibility of estimating the kinetic constants. The model (Eqs. 6a and 6b) involves four constants: $\bar{\alpha}$, $\bar{\beta}$, ν_a, and ν_d. However, the fitting of the equilibrium data gives a relationship between $\bar{\alpha}$ and $\bar{\beta}$, and ν_a and ν_d, thus leaving two kinetic constants as undetermined. To simplify the analysis, however, the dependence of activation energies on the surface coverage will be neglected, and the simplified Langmuir kinetics will be used. A Langmuir fit has already been shown for the equilibrium data (Figure 7); using this type of kinetics to describe unsteady sorption, coupled with bulk diffusion, involves only one unknown kinetic constant. Detailed in Figure 10 are theoretical curves of the surface tension relaxation in dimensional time for the diffusion-limited model and for several finite values of $\bar{\beta}$ for $C_o = 9.89 \times 10^{-9}$ mol/cm³ and $D = 2.6 \times 10^{-6}$ cm²/s. Comparing the finite $\bar{\beta}$ curves to the diffusion-limited relaxation, it is clear that $\bar{\beta}$ is at least as large as O (5×10^7 cm³ · mol^{-1} · s^{-1}), and a corresponding lower bound for $\bar{\alpha}$ ($= a\bar{\beta}$) is of the order 10^{-2} s^{-1}.

Discussion and Concluding Remarks

The technique of pendant drop tensiometry enhanced by video imaging is an effective tool for studying the unsteady adsorption of surfactant molecules onto both a liquid/gas and a liquid/liquid interface. In principle, the technique is applicable to the study of the adsorption process of any surface-active molecule onto a fluid surface as long as the surface activity is strong enough to appreciably lower the surface tension and the bulk concentration is not too high to make a large diffusional flux complete the surface adsorption too quickly.

To obtain quantitative information about the relaxation, the equilibrium adsorption must first be fitted using an isotherm [i.e., $\gamma = f(C_o)$]. This isotherm is then used later in the

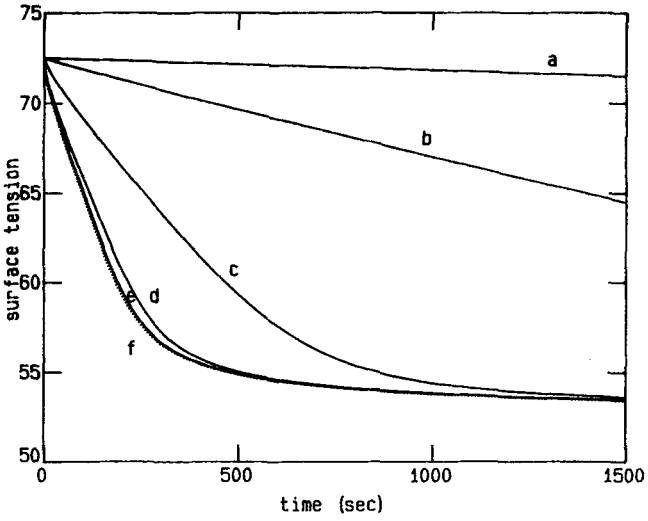

Figure 10. Numerical solutions for surface tension as a function of time for the mixed transport equation.

β = (a) 10^4, (b) 10^5, (c) 10^6, (d) 10^7, (e) 5×10^7 ($cm^3 \cdot mol^{-1} \cdot s^{-1}$), and (f) diffusion-limited (·····). C_o = 9.89×10^{-9} mol/cm^3 (γ = mN/m)

theoretical modeling to obtain the surface tension at a particular point in time in terms of the subsurface concentration at that time [i.e., $\gamma(t) = f(C_s(t))$]. This is a particularly crucial step, since if the model fitting of the data were poor, then the value of γ which the model assigns to a particular C_s will be in error. Here, a Langmuir formalism was used, in which the activation energies for adsorption and desorption depend on the surface coverage (Eqs. 6–8). It was found that by including the dependence of the activation energies on Γ, a much better fit of the equilibrium data at low concentrations was achieved. The value of k for the Triton X-100 molecule, which best fits the equilibrium data, is positive and equal to 2.52. It should be noted that the use of this type of isotherm, in which activation energies are surface-concentration-dependent, is restricted to values of k larger than -4. For values of k less than this critical one, there exists a bulk concentration for which $\partial\Gamma/\partial C$ becomes infinite and a region for which $\partial\gamma/\partial\Gamma$ becomes positive.

The agreement achieved between the theoretical and experimental relaxations by varying the diffusion coefficient is, on the average, fairly good as reflected by the small values of the standard error at the optimum D (cf. Figure 8). A careful examination of the fits at various bulk concentrations reveals that the deviation between the theoretical and experimental curves increases with the bulk concentration (see also Figure 8) and that this deviation occurs principally during the middle time interval. In this middle interval the relaxation in the experimental surface tension appears to decelerate. The reasons for this behavior are not completely clear, but it may be conjectured that the slow experimental relaxation during the middle interval is due to the fact that the population distribution of n (the number of ethoxy groups) of the Triton X-100 used is not extremely sharp (cf. a discussion of the molecular weight distribution of Triton X-100 by Rouviere et al., 1989). In this case, there is more than one adsorbing species; each species, though most likely having the same diffusion coefficient, has different surface activities because of differing numbers of ethoxy groups. Miller et al. (1979) has examined theoretically the unsteady adsorption of two surfactants with differing surface activity and equal diffusivities. He finds that decelerations and/or plateau behavior in the surface tension relaxation can occur at the middle time intervals, if the surface activities (as measured by the Langmuir-von Szyskowski constant a) differ by an order of magnitude or more.

The use of the data of the entire relaxation curve is important in obtaining the diffusion coefficient. As noted in the Introduction section, most studies use a simpler procedure, in which only the short or long contact time experimental data are compared with theoretical constructs. Consider the exclusive use of the short contact time data. As is well known, as $t \to 0$, the diffusion-controlled expression of Eq. 5 indicates that Γ increases as $\sqrt{t}$:

$$\Gamma(t) \approx 2\left(\frac{D}{\pi}\right)^{1/2} C_o \sqrt{t} \qquad (t \to 0) \tag{11}$$

The usual approach is to first convert the surface tension relaxation data into a temporal profile of surface concentration by using the equilibrium isotherm, then plot the short time (concentration) values with $\sqrt{t}$, and finally by fitting a straight line through the data, obtain D from the slope using the above equation. If this data reduction were applied, for example, to the short time relaxation profiles of the bulk concentrations of 1.55×10^{-9} and 9.89×10^{-9} mol/cm^3 (cf. Figure 4), the short time surface concentration data fall correctly on straight lines in $\sqrt{t}$, and the average diffusion coefficient is fairly close (2.9×10^{-6} cm^2/s as opposed to 2.6×10^{-6} cm^2/s), but the standard deviation is 0.7×10^{-6} cm^2/s as opposed to 0.14×10^{-6} cm^2/s. The larger standard deviation reflects the fact that the short time approach is not reproducible because fewer points are used and that the short time data are influenced greatly by variable initial conditions such as momentary convection and initial adsorption during the drop creation period. The short time method has another drawback: as the numerical solution of Eqs. 5 and 7 shows, the departure of the exact solution from the approximate one as given in Eq. 11 becomes larger than 5% when Γ/Γ_o exceeds 0.1 for $C_o = 1.55 \times 10^{-9}$ mol/cm^3 and 0.4 for $C_o = 9.89 \times 10^{-9}$ mol/cm^3. As C_o further increases, the cutoff value for Γ/Γ_o for an error of less than 5% increases to approximately 0.8, but at these higher concentrations the adsorption proceeds too quickly to obtain enough data points corresponding to $\Gamma/\Gamma_o < 0.8$. For example, in the data taken in this study, except for the two lowest concentrations (1.55×10^{-9} and 9.89×10^{-9} mol/cm^3), the relaxation proceeded too quickly to obtain enough data points which could be used with the short time approximation. Nevertheless, the use of the remaining relaxation profile at higher concentrations (1.55×10^{-8} and 2.32×10^{-8} mol/cm^3) yielded more accurate values for the diffusion coefficient when compared to the numerical solution for the entire relaxation.

Acknowledgment

This work was supported in part by a grant from the Engineering Research Program of the Office of Basic Energy Science of the Department of Energy (DE-FG02-88ER13820).

Notation

a = Langmuir-von Szyskowski constant, mol/cm^3
b = radius of spherical drop
b_1, b_2 = constants defined by Eq. 10
$B = \Delta\rho\, g\, R_0^2/\gamma$ (Bond number)
C = bulk concentration, mol/cm^3
C_o = concentration far from the drop, mol/cm^3
C_s = subsurface concentration, mol/cm^3
$C_s' = C_s/C_o$
D = diffusion coefficient, cm/s^2
d_e = equatorial diameter
d_n = normal distance between measured point and calculated curve
d_s = diameter in a selected plane at a distance d_e from the apex
E = objective function
E_a, E_d = energy of activation for adsorption and desorption
E_a^0, E_d^0 = activation energies in kinetic adsorption equation
g = gravitational acceleration constant
$h = \Gamma_o/C_o$, adsorption depth
$H = -\beta(d_e/R_o)^2$
$J_o(x)$ = Bessel function of the first kind
$k = (\nu_a - \nu_d)\Gamma_\infty/RT$
N = total number of experimental points
ΔP = pressure drop across the curved interface
q_i = variables of objective function
r = radial coordinate
r_s = ratio of curvature term
R = gas constant
R_o = radius of apex
R_1, R_2 = principal radii of curvature of the surface
s = arc length from apex
$s' = s/R_o$
$S = d_s/d_e$
t = time
$t' = tD/h^2$
$t_n = n\delta$
T = temperature
u_n = measured point
v = calculated curve
x, z = spatial coordinate
$x', z' = x/R_o, z/R_o$, nondimensional spatial coordinate
X_o, Z_o = location of apex
$y = \Gamma/\Gamma_\infty$

Greek letters

α, β = preexponential factors
$\bar{\alpha}, \bar{\beta}$ = ratio of adsorption and desorption rates as defined after Eq. 7
γ = surface tension, mN/m
γ_o = clean surface tension, mN/m
γ_e = equilibrium surface tension, mN/m
Γ = surface concentration, mol/cm^2
$\Gamma' = \Gamma/\Gamma_o$
Γ_o = equilibrium surface concentration, mol/cm^2
Γ_∞ = maximum surface concentration, mol/cm^2
δ = step size of integration
ν_a, ν_d = coefficients appearing in activation energy expression
π = 3.14159
$\Delta\rho$ = density difference between the fluids
τ = dummy variable
ϕ = turning angle

Literature Cited

Adamczyk, Z., and J. Petlicki, "Adsorption and Desorption Kinetics of Molecules and Colloidal Particles," *J. Colloid Interf. Sci.*, **118,** 20 (1987).

Ambwani, D. S., and T. Fort, Jr., "Pendant Drop Technique for Measuring Liquid Boundary Tensions," *Surface and Colloid Science,* R. J. Good and R. R. Stromberg, eds., Vol. 11, p. 93, Plenum, New York (1979).

Andreas, J. M., E. A. Hauser, and W. B. Tucker, "Boundary Tension by Pendant Drops," *J. Phys. Chem.*, **42,** 1001 (1938).

Balbaert, I., G. Bleys, and P. Joos, "Measurement of the Dynamic Surface Tension in an Asymmetric Free-Falling Film," *J. Colloid Interf. Sci.*, **115,** 362 (1987).

Bendure, R. L., "Dynamic Surface Tension Determination with the Maximum Bubble Pressure Method," *J. Colloid Interf. Sci.*, **35,** 238 (1971).

Borwankan, R. P., and D. T. Wasan, "The Kinetics of Adsorption of Surface-Active Agents at Gas-Liquid Surfaces," *Chem. Eng. Sci.*, **38,** 1637 (1983).

Defay, R., and R. Hommelen, "Measurement of Dynamic Surface Tension of Aqueous Solutions by the Oscillating Jet Method," *J. Colloid Sci.*, **13,** 553 (1958).

Fainerman, V. B., "Kinetics of Adsorption from Solution at a Deformable Liquid Interface," *Kolloidn. Zh.*, **42,** 96 (1980).

Fainerman, V. B., and S. V. Lylyk, "Dynamic Surface Tension and Kinetics of Adsorption in Solutions of Nomal Alcohols," *Kolloidn. Zh.*, **44,** 598 (1982).

Girault, H. H. J., D. J. Schiffrin, and B. D. V. Smith, "Drop Image Processing for Surface and Interfacial Tension Measurements," *J. Electr. Chem.*, **137,** 207 (1982).

———, "The Measurement of Interfacial Tension of Pendant Drops Using a Video-Image Profile Digitizer," *J. Colloid Interf. Sci.*, **101,** 257 (1984).

Guzman, R. Z., R. G. Carbonell, and P. K. Kilpatrick, "The Adsorption of Proteins to Gas-Liquid Interfaces," *J. Colloid Interf. Sci.*, **114,** 536 (1986).

Hansen, R. S., M. E. Purchase, T. C. Wallace, and R. W. Woody, "Extension of the Vibrating Jet Method for Surface Tension Measurement to Jets of Non-Uniform Velocity Profiles," *J. Phys. Chem.*, **62,** 210 (1958).

Hua, X. Y., and M. J. Rosen, "Dynamic Surface Tension of Aqueous Surfactant Solutions," *J. Colloid Interf. Sci.*, **124,** 652 (1988).

Huh, C., and R. L. Reed, "A Method for Estimating Interfacial Tensions and Contact Angles from Sessile and Pendant Drop Shapes," *J. Colloid Interf. Sci.*, **91,** 472 (1983).

Joos, P., and E. Rillaerts, "Theory on the Determination of the Dynamic Surface Tension with the Drop Volume and Maximum Bubble Pressure Methods," *J. Colloid Interf. Sci.*, **79,** 96 (1981).

Kloubek, J., "Measurement of the Dynamic Surface Tension by the Maximum Bubble Pressure Method," *J. Colloid Interf. Sci.*, **41,** 17 (1972).

Lucassen, J., and M. van den Tempel, "Dynamic Measurements of Dilational Properties of a Liquid Interface," *Chem. Eng. Sci.*, **27,** 1283 (1972).

———, "Longitudinal Waves on Visco-Elastic Surfaces," *J. Colloid Interf. Sci.*, **41,** 491 (1972).

Lucassen-Reynders, E. H., and M. van den Tempel, "Surface Equation of State for Adsorbed Surfactants," *Proc. Int. Cong. Surface Activity,* Brussels, Vol. B, p. 779, Gordon & Breach, New York (1964).

Lunkenheimer, K., and K.-D. Wantke, "Determination of the Surface Tension of Surfactant Solutions Applying the Method of Lecomte du Nouy (Ring Tensiometer)," *Coll. Polym. Sci.*, **259,** 354 (1981).

Lunkenheimer, K., C. Hartenstein, R. Miller, and K.-D. Wantke, "Investigations of the Method of the Radially Oscillating Bubble," *Colloids and Surf.*, **8,** 271 (1984).

Lunkenheimer, K., G. Serrien, and P. Joos, "The Adsorption Kinetics of Octanol at the Air/Solution Interface Measured with the Oscillating Bubble and Oscillating Jet Methods," *J. Colloid Interf. Sci.*, **134,** 407 (1990).

Miller, R., and G. Kretzschmar, "Numerische Losung Fur ein gemischtes Modell der diffusions-kinetik-kontrollierten Adsorption," *Coll. Polym. Sci.*, **258,** 85 (1980).

Miller, R., and K. Lunkenheimer, "Adsorption Kinetics Measurements of Some Nonionic Surfactants," *Coll. Polym. Sci.*, **264,** 357 (1986).

Miller, R., K. Lunkenheimer, and G. Kretzschmar, "Ein Modell Fur die diffusionskontrollierte Adsorption von Tensidgemisxhen an fluiden Phasengrenzen," *Coll. Polym. Sci.*, **257,** 1118 (1979).

Miller, R., and K.-H. Schano, "Adsorption Kinetics of Nonionic Surfactants using the Drop Volume Method," *Coll. Polym. Sci.*, **264,** 277 (1986).

Misak, M. D., "Equations for Determining $1/H$ versus S Values in

Computer Calculations of Interfacial Tension by the Pendant Drop Method," *J. Colloid Interf. Sci.*, **27**, 141 (1968).
Mysels, K. J., "Diffusion-Controlled Adsorption Kinetics: General Solution and Some Applications," *J. Phys. Chem.*, **86**, 4648 (1982).
Noskov, B. A., and A. A. Vasil'ev, "Waves on the Surface of Solutions of Surfactants," *Kolloidn. Zh.*, **50**, 909 (1988).
Pierson, F. W., and S. Whitaker, "Studies of the Drop-Weight Method for Surfactant Solutions," *J. Colloid Interf. Sci.*, **54**, 203 (1976).
Rotenberg, Y., L. Barouka, and A. W. Neumann, "Determination of Surface Tension and Contact Angle from the Shapes of Axisymmetric Fluid Interfaces," *J. Colloid Interf. Sci.*, **93**, 169 (1983).
Rouviere, J., J. L. Razakarison, J. Marignan, and B. Brun, "Rheological and X-Ray Studies on Nonionic Surfactant Emulsions Involving Hydrocarbon or Silicone Oil," *J. Colloid Interf. Sci.*, **133**, 293 (1989).
Thomas, W. D. E., and L. Potter, "Solution/Air Interfaces. An Oscillating Jet Relative Method for Determining Dynamic Surface Tensions," *J. Colloid Interf. Sci.*, **50**, 397 (1975).
van den Tempel, M., and E. H. Lucassen-Reynders, "Relaxation Processes at Fluid Interfaces," *Adv. Colloid Interf. Sci.*, **18**, 281 (1983).
Van der Bogaert, R., and P. Joos, "Dynamic Surface Tensions of Sodium Myristate Solutions," *J. Phys. Chem.*, **83**, 2244 (1979).
Van hunsel, J., G. Bleys, and P. Joos, "Adsorption Kinetics at the Oil/Water Interface," *J. Colloid Interf. Sci.*, **114**, 432 (1986).
Van hunsel, J., and P. Joos, "Steady-State Dynamic Interfacial Tensions of 1-Alkanols during Mass Transfer across the Hexane/Water Interface," *Langmuir*, **3**, 1069 (1987).
———, "Study of Dynamic Interfacial Tension at the Oil/Water Interface," *Coll. Polym. Sci.*, **267**, 1026 (1989).
Ward, A. F. H., and L. Tordai, "Time-Dependence of Boundary Tensions of Solutions," *J. Chem. Phys.*, **14**, 453 (1946).
Weast, R. C., *Handbook of Chemistry and Physics*, 53rd ed., Chemical Rubber Co. (1973).

Manuscript received Feb. 23, 1990, and revision received Sept. 25, 1990.